

# Exciton delocalization in the antenna of purple bacteria: Exciton spectrum calculations using X-ray data and experimental site inhomogeneity

Tatiana V. Dracheva<sup>a</sup>, Vladimir I. Novoderezhkin<sup>a,b</sup>, Andrei P. Razjivin<sup>a,\*</sup>

<sup>a</sup>International Laser Center, Moscow State University, Moscow 119899, Russian Federation

<sup>b</sup>Scientific Research Center on Technological Lasers, Russian Academy of Science, Troitzk, Moscow Region, Russian Federation

Received 5 April 1996

**Abstract** Electron absorption and circular dichroism spectra of the peripheral light-harvesting complex (LH2) of photosynthetic purple bacteria were calculated taking into account the real-life spatial arrangement and experimental inhomogeneous broadening of bacteriochlorophyll molecules. It was shown that strong excitonic interactions between 18 bacteriochlorophyll molecules (BChl850) within the circular aggregate of the LH2 complex result in an exciton delocalization over all these pigment molecules. The site inhomogeneity (spectral disorder) practically has no influence on exciton delocalization. The splitting between two lowest exciton levels corresponds to experimentally revealed splitting by hole-burning studies of the LH2 complex.

**Key words:** Exciton interaction; Bacterial photosynthesis; Inhomogeneous broadening; Absorption spectrum; CD spectrum; LH2 complex

## 1. Introduction

Nowadays there are two theoretical models describing spectral and kinetic properties of the light-harvesting antenna and reaction centers of purple photosynthetic bacteria. The first model assumes an excitation localization at the BChl dimer (or small cluster of strongly coupled BChls) and treats the energy transfer processes as a hopping of such localized excitation between weakly coupled dimers (clusters). This model is widely accepted and used up to now [1,2]. Another model assumes exciton delocalization over the circular aggregate of strongly coupled BChls with  $C_N$  symmetry, where  $N$  is the number of BChl monomers in the LH1 or LH2 complex [3–6].

Previously we analyzed the circular aggregate as a model of the antenna of purple bacteria. According to this model light-harvesting BChl molecules are spectrally identical and are arranged in the form of a perfect ring with  $C_N$  symmetry. This idealized model is in good agreement with experimental results including those which are sensitive to the aggregate's form and size (picosecond absorbance difference spectra [5] and hole-burning spectra [7]).

Recently the precise spatial arrangement of BChl molecules in the light-harvesting complex LH2 has become available due to X-ray investigations [8]. According to these data the real-life aggregate structure has  $C_{N/2}$  symmetry. This permits us to

test the validity of our previous predictions on the basis of our idealized model [3–6]. It is important to elucidate the difference between exciton spectra of the real-life aggregate structure with the  $C_{N/2}$  symmetry and those of the idealized model with  $C_N$  symmetry.

Also it is important to investigate the influence of spectral inhomogeneity on the exciton states. Generally spectral inhomogeneity can significantly break delocalized exciton states. Strong inhomogeneity can lead to localized exciton formation. The fact that spectral lines are inhomogeneously broadened is usually treated as an indication of excitation localization in the antenna [1,2].

In this paper exciton states were calculated for the real-life LH2 antenna taking into account the spatial BChl arrangement and experimental values of spectral inhomogeneity. It was shown that site inhomogeneity has almost no effect on exciton delocalization. The calculated exciton structure of LH2 complex is in agreement with the hole-burning data.

## 2. Spatial structure of the light-harvesting complex

According to X-ray data [8] the antenna complex LH2 from *Rhodospirillum rubrum* consists of 18 BChl molecules (spectral form B850), which form the perfect ring with  $C_9$  symmetry (two molecules in the unit cell). The orientation of transition dipole moments of BChl molecules is shown at Fig. 1. The Mg–Mg distances between the nearest neighboring BChl850 molecules are 0.87 nm and 0.97 nm. The energies of interaction between the nearest neighboring molecules in the point dipole approximation are equal to  $M_0 = 785 \text{ cm}^{-1}$  and  $M_1 = 566 \text{ cm}^{-1}$  for intermolecular distances of 0.87 nm and 0.97 nm, respectively, and a dipole strength of a BChl molecule of 60 (debye)<sup>2</sup> according to Pearlstein [9].

## 3. Exciton structure with regard to the spectral disorder

The method of exciton structure calculation for the circular aggregate with spectral disorder was developed in [6]. An analytical solution of this problem can be obtained using perturbation theory in the case of weak disorder [4,6,7]. In this paper we analyzed the exciton structure for an arbitrary disorder value by the same method using numerical calculations. The numerical diagonalization of the Hamiltonian was performed assuming that the energy distribution of molecules has gaussian statistics without intersite correlation. The site inhomogeneity may be characterized by the width (FWHM) of this distribution,  $\Gamma$ .

The inhomogeneously broadened spectra were simulated without taking into account the homogeneous line broadening. The results for different values of  $\Gamma$  are shown in Table 1 (the position and intensity of exciton components in the absorbance and CD spectra) and in Fig. 2 (the inhomogeneous

\*Corresponding author: Fax: (7) (095) 939 3181.  
E-mail: razjivin@beloz.genebee.msu.ru

Abbreviations: BChl, bacteriochlorophyll

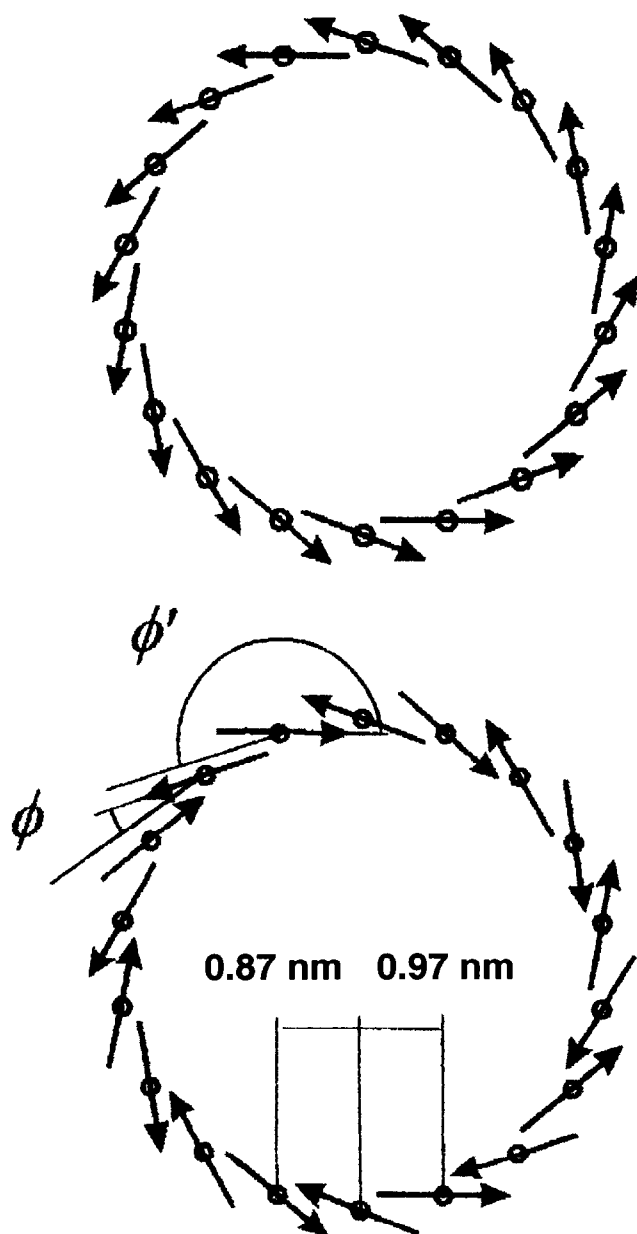


Fig. 1. A model of the circular aggregate with  $C_{18}$  symmetry (top) and with  $C_9$  symmetry (bottom) including 18 BChl molecules. The dipole moments of  $Q_y$  transition are shown by arrows.  $\phi$  and  $\phi'$  are the angles between the projection of the transition dipoles on the circle plane and the tangent to the circle.  $\phi$  and  $\phi'$  are the angles between the transition dipoles and the circle plane (not shown). According to [8]  $\phi=20^\circ$ ;  $\phi'=200^\circ$ ;  $\phi=10^\circ$ ;  $\phi'=5^\circ$ .

line shapes of absorption spectra) and Fig. 3 (the inhomogeneous line shapes of CD spectra).

In the case of the  $C_9$  symmetry ring with 18 molecules there are two exciton level sets (two Davydov components each of 9 levels:  $k_-$  and  $k_+$  are equal to 0,  $\pm 1$ ,  $\pm 2$ ,  $\pm 3$ ,  $\pm 4$  where  $k_-$  and  $k_+$  wave numbers correspond to lower and higher Davydov components).

The structure of the lower (red shifted) Davydov component is the same as for the single ring with one molecule in the unit cell. It consists of a strong line corresponding to the two-fold degenerated level  $k_- = \pm 1$  and a weak long-wavelength

line corresponding to the  $k_- = 0$  level. Transitions to  $k_- = \pm 1$  and  $k_- = 0$  levels have circular polarization in the ring plane and linear polarization normal to the ring plane [3,4]. These  $k_- = \pm 1$  and  $k_- = 0$  levels produce a two-component CD spectrum that is the same as for the single ring. The splitting between levels  $k=0$  and  $k=\pm 1$  in the limit case  $M_0=M_1=M$  is the same as for the single ring of 18 molecules with the  $C_{18}$  symmetry.

The exciton levels of the upper (blue shifted) Davydov component gives no contribution to absorption and CD spectra except a weak line corresponding to the  $k_+ = 0$  level.

So, the exciton structure of the double ring (two molecules in the unit cell), which corresponds to the real-life structure, is approximately the same as for the single ring of 18 BChls.

For the homogeneous double ring,  $\Gamma = 0$ , the intensity of the upper linearly polarized level  $k_+ = 0$  is 10-fold stronger than that of the lowest,  $k_- = 0$ . However, even for moderate inhomogeneity (about  $\Gamma = 90 \text{ cm}^{-1}$ ) these intensities in absorption spectra become approximately equal due to exciton wave function mixing. Further inhomogeneity growth produces a further increase of lower level intensity due to mixing with strong lines  $k_- = \pm 1$ . For  $\Gamma = 470 \text{ cm}^{-1}$  the  $k_- = 0$  level is 10-fold stronger than the  $k_+ = 0$  level. For this inhomogeneity value the  $k_- = \pm 2$  levels become dipole allowed due to mixing with  $k_- = \pm 1$ . However, the intensity of strong lines  $k_- = \pm 1$  decreases not more than for 20%. So, the influence of energy disorder on dipole moments of exciton states is small in this range of  $\Gamma$ . It means that there is no significant destruction of delocalized exciton states. That is why the region  $\Gamma = 0\text{--}500 \text{ cm}^{-1}$  may be treated as the region of weak inhomogeneity.

However, the shift of  $k_- = 0$ ,  $k_- = 1$  and  $k_- = -1$  lines, absolute and relative to each other, is significant in this range. The splitting between the  $k_- = 0$  level and  $k_- = 1$  and  $k_- = -1$  levels is equal to  $78 \text{ cm}^{-1}$  and  $78 \text{ cm}^{-1}$  for  $\Gamma = 0$  and  $98 \text{ cm}^{-1}$  and  $170 \text{ cm}^{-1}$  for  $\Gamma = 467 \text{ cm}^{-1}$ .

Within the range  $0 \leq \Gamma \leq 500 \text{ cm}^{-1}$  the inhomogeneous width of exciton levels  $\Gamma_{\text{ex}}$  is less than  $\Gamma$  by a factor of  $\sqrt{2N}$  (exchange narrowing factor), that is  $\Gamma_{\text{ex}} = 0\text{--}120 \text{ cm}^{-1}$ . The inhomogeneous width is comparable with the splitting between the

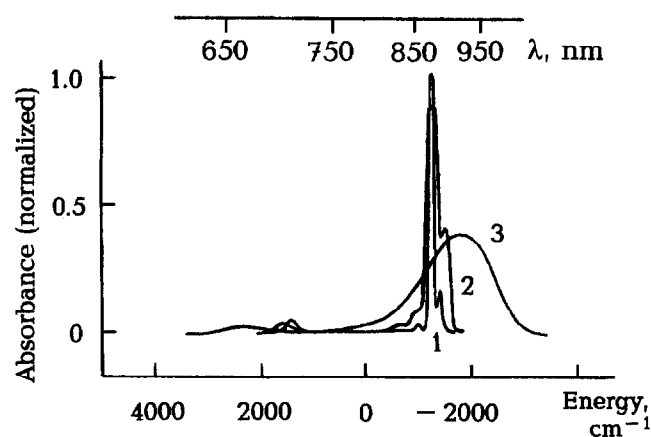


Fig. 2. The inhomogeneously broadened exciton components of absorption spectra for the circular aggregate with  $C_9$  symmetry (18 BChl molecules) for different site inhomogeneity values  $\Gamma$  (the homogeneous broadening of exciton levels was not taken into account). Curves 1, 2 and 3 correspond to  $\Gamma$  values equal to  $185 \text{ cm}^{-1}$ ,  $740 \text{ cm}^{-1}$  and  $1850 \text{ cm}^{-1}$ , respectively. The zero of energy is taken equal to the electronic excitation energy of the BChl monomer.

three lowest levels ( $k_- = 0, -1, +1$ ) but does not exceed the splitting between them and the higher exciton levels ( $k_- = -2, +2$ , etc.). The spectrum consists of three intensive components ( $k_- = 0, -1, +1$  levels) which are partially overlapped and more weak blue shifted components (Fig. 2). At room temperature (about  $200 \text{ cm}^{-1}$ ) only the strongest levels  $k_- = 0, -1, +1$  will be populated. In this case the exciton dynamics will be not significantly different from that of the homogeneous aggregate.

When  $\Gamma > 500 \text{ cm}^{-1}$  the intensity of the  $k_- = 0$  level and upper  $k_- = \pm 2, k_- = \pm 3$ , etc. levels increases due to the  $k_- = \pm 1$  level. For  $\Gamma = 900 \text{ cm}^{-1}$  the dipole strength of the  $k_- = \pm 1$  line contains not more than 60% of the whole aggregate dipole strength. The radius of exciton delocalization is significantly reduced.

For  $\Gamma = 1800 \text{ cm}^{-1}$  the distribution of dipole strength over exciton levels tends to a more uniform one. The inhomogeneous width of individual exciton levels significantly exceeded the splitting between them in this case. As a result the exciton components of the spectrum are not resolved even without taking into account a homogeneous broadening of upper levels. This is a case of exciton localization on few molecules of the aggregate. The limit of uniform distribution corresponds to excitation localization at one molecule. However, this is not true even for very high  $\Gamma$  values.

It is interesting that a CD spectrum has a two-component form with a broad asymmetrical peak at the short-wavelength side for all investigated disorder values (Fig. 3). The contribution of the upper Davydov component is not substantial.

#### 4. Discussion

The energy disorder does not significantly influence the delocalized exciton states in the LH2 complex if  $\Gamma < 500 \text{ cm}^{-1}$  or  $\Gamma_{\text{ex}} < 120 \text{ cm}^{-1}$ . One can assume that the critical value of  $\Gamma_{\text{ex}}$  which characterizes a threshold for delocalized exciton destruction is  $\Gamma_{\text{ex}}^{\text{cr}} = 120 \text{ cm}^{-1}$ . This critical value is convenient to compare with the experimental value  $\Gamma_{\text{ex}}$ , which can be

estimated from hole-burning data [10–12], site-selective fluorescence spectroscopy [13], disperse kinetics of fluorescence and/or induced absorbance changes [1,14].

The  $\Gamma_{\text{ex}}$  value obtained by hole-burning spectroscopy at 4.2 K is equal to  $60 \text{ cm}^{-1}$  for *Rhodobacter sphaeroides* LH2 and  $110 \text{ cm}^{-1}$  for LH2 complex from *R. acidophila* [10–12].

One can see that for both complexes  $\Gamma_{\text{ex}}$  values do not exceeded  $\Gamma_{\text{ex}}^{\text{cr}} = 120 \text{ cm}^{-1}$ . In other words, the site inhomogeneity value for LH2 complexes from purple bacteria fits the region of weak inhomogeneity. In this region the influence of disorder mainly results in a shift of exciton levels without significant changes in their wave functions, dipole strengths and effective delocalization radius. This is followed by significant inhomogeneous line broadening but the structure of delocalized exciton states still remains unperturbed. So, delocalized states are a good basis for the description of exciton dynamics in these complexes. When only one exciton level is populated (at low temperature), the exciton state wave function is uniform, i.e. the exciton radius is equal to the total number of molecules  $N$ . At room temperature several exciton levels are populated ( $k_- = 0$  and  $k_- = \pm 1$  for our parameter set). Superposition of exciton states results in a non-uniform distribution of exciton density. The effective exciton radius is less than  $N$  (by a factor of 1.5–2), but still remains very large. The exciton radius reduction due to superposition of exciton states at finite temperature is a common feature for both homogeneous and inhomogeneous aggregates. An additional reason for exciton radius reduction is site inhomogeneity. In this paper we demonstrated that its influence in real-life BChl aggregates is weak. It means that all specific exciton effects predicted by the standard theory for a homogeneous aggregate (see our previous papers [3–6]) will take place in natural BChl aggregates.

One can compare the splitting between the two lowest exciton levels according to calculations and experimental data. The experimental hole-burning spectrum for the antenna LH2 complex from *R. acidophila* has two peaks at  $11470 \text{ cm}^{-1}$  (871.8 nm) and  $11320 \text{ cm}^{-1}$  (883.4 nm) within the B850

Table 1

The dependences of spectral position and intensity of exciton components in the absorbance spectrum and CD of the circular aggregate with  $C_9$  symmetry containing 18 BChl molecules on the spectral disorder value

$k_{\pm}$	$\Gamma=0$			$\Gamma=467$			$\Gamma=1850$		
	$E_k^{\pm}$	$A_k^{\pm}$	$C_k^{\pm}$	$E_k^{\pm}$	$A_k^{\pm}$	$C_k^{\pm}$	$E_k^{\pm}$	$A_k^{\pm}$	$C_k^{\pm}$
$k_- = 0$	-1351	0.014	-2.410	-1427	0.746	-1.380	-1843	1.038	-0.340
$k_- = -1$	-1271	2.940	1.178	-1329	2.281	0.524	-1587	1.150	0.017
$k_- = +1$	-1271	2.940	1.178	-1257	2.347	0.681	-1394	1.071	0.109
$k_- = -2$	-1044	0	0	-1089	0.214	0.035	-1201	0.792	0.071
$k_- = +2$	-1044	0	0	-1013	0.180	0.027	-1034	0.543	0.040
$k_- = -3$	-701	0	0	-742	0.039	0.002	-814	0.343	0.030
$k_- = +3$	-701	0	0	-667	0.034	0.003	-628	0.249	0.006
$k_- = -4$	-318	0	0	-355	0.015	0.001	-381	0.159	0.004
$k_- = +4$	-318	0	0	-274	0.015	0.001	-161	0.130	0.013
$k_+ = +4$	318	0	0	269	0.005	0.000	166	0.072	0.001
$k_+ = -4$	318	0	0	352	0.005	0.000	379	0.065	0.000
$k_+ = +3$	701	0	0	662	0.004	0.000	632	0.047	0.001
$k_+ = -3$	701	0	0	739	0.004	0.001	828	0.036	0.000
$k_+ = +2$	1044	0	0	1007	0.004	0.001	1041	0.035	0.003
$k_+ = -2$	1044	0	0	1086	0.005	0.002	1210	0.035	0.014
$k_+ = +1$	1271	0	0	1254	0.013	0.009	1402	0.036	0.008
$k_+ = -1$	1271	0	0	1327	0.018	0.011	1596	0.043	0.003
$k_+ = 0$	1351	0.106	0.054	1421	0.073	0.031	1851	0.061	0.023

The energies of levels  $E_k^{\pm}$  (in  $\text{cm}^{-1}$ ) were measured from  $\Delta E$ . The width of inhomogeneous distribution of molecular energy  $\Gamma$  is also given in  $\text{cm}^{-1}$ . Intensities  $A_k^{\pm}$  and  $C_k^{\pm}$  are given in arbitrary units.

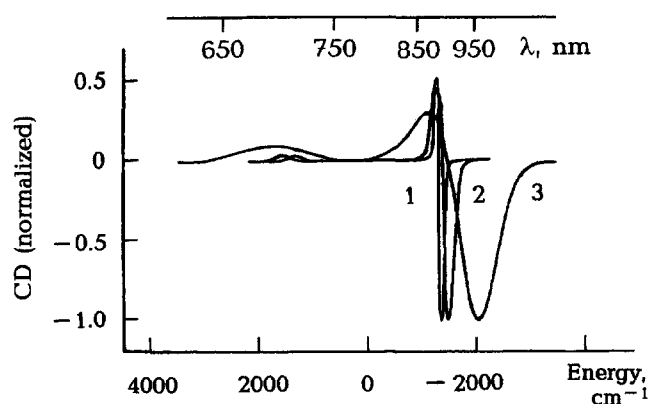


Fig. 3. The inhomogeneously broadened exciton components of CD spectra for the circular aggregate with  $C_9$  symmetry (18 BChl molecules) for different site inhomogeneity values  $\Gamma$ . All parameters are as in Fig. 2.

band [12]. According to our model the frequency  $11\,320\text{ cm}^{-1}$  may be ascribed to the  $k_{-}=0$  level that contributes to narrow zero-phonon peaks in hole-burning spectra. Then the frequency  $11\,470\text{ cm}^{-1}$  will correspond to  $k_{-}=\pm 1$  levels broadened due to relaxation that gives rise to a broad hole. The inhomogeneous width of the lower level ( $11\,320\text{ cm}^{-1}$ ) is equal to  $\Gamma_{\text{ex}}=110\text{ cm}^{-1}$  corresponding to  $\Gamma=467\text{ cm}^{-1}$ .

According to our calculations for  $\Gamma=467\text{ cm}^{-1}$  the spectrum consists of a weak  $k_{-}=0$  line and strong  $k_{-}=1$  and  $k_{-}=-1$  lines shifted by  $98\text{ cm}^{-1}$  and  $170\text{ cm}^{-1}$  with respect to the lowest level (see Table 1). Being broadened due to relaxation  $k_{-}=\pm 1$  levels produce a broad band shifted by  $134\text{ cm}^{-1}$  with respect to the lowest  $k_{-}=0$  level. This estimated value corresponds closely to the difference between the peaks of the hole-burning spectrum:  $11\,470\text{ cm}^{-1}-11\,320\text{ cm}^{-1}=150\text{ cm}^{-1}$ .

So we can conclude that the calculated exciton level energies are in good agreement with the splitting between spectral components in hole-burning profiles for the LH2 complex.

In conclusion, spectral disorder only slightly reduces the radius of delocalized excitons at least in the peripheral antenna of purple bacteria. That is why the model of a spectrally homogeneous aggregate can be used for a qualitative description of exciton dynamics in this antenna. Moreover, one can use the more convenient single ring model because the differ-

ences of exciton structure between single ring and double ring aggregates are minor. So, our calculations according to the model of spectrally homogeneous single ring aggregates published earlier [3–6] are correct at least as a qualitative description.

For a more correct quantitative description of spectra and exciton dynamics of the antenna of purple bacteria the real structure and spectral disorder information should be used. It is specially important, for example, for fluorescence anisotropy, which is sensitive to the wave function of the lowest exciton level. As was shown in this paper, even weak spectral disorder may result in significant relative variations of dipole strength (and especially dipole moment vector).

**Acknowledgements:** The present research was made possible in part by Grant No. 6.1.2.3 from the Russian programme 'Laser physics and laser systems'.

## References

- [1] Pullerits, T., Visscher, K.J., Hess, S., Sundstrom, V., Freiberg, A., Timpmann, K. and van Grondelle, R. (1994) *Biophys. J.* 66, 236–248.
- [2] Somsen, O.J.G., van Mourik, F., van Grondelle, R. and Valkunas, L. (1994) *Biophys. J.* 66, 1580–1596.
- [3] Novoderezhkin, V.I. and Razjivin, A.P. (1993) *FEBS Lett.* 330, 5–7.
- [4] Novoderezhkin, V.I. and Razjivin, A.P. (1994) *Photosynthesis Res.* 42, 9–15.
- [5] Novoderezhkin, V.I. and Razjivin, A.P. (1995) *FEBS Lett.* 368, 370–372.
- [6] Novoderezhkin, V.I. and Razjivin, A.P. (1995) *Biophys. J.* 68, 1089–1100.
- [7] Dracheva, T.V., Novoderezhkin, V.I. and Razjivin, A.P. (1995) *Chem. Phys.* 194, 223–235.
- [8] McDermott, G., Prince, S.M., Freer, A.A., Hawthornthwaite-Lawless, A.M., Papiz, M.Z., Cogdell, R.J. and Isaacs, N.W. (1995) *Nature* 374, 517–521.
- [9] Pearlstein, R.M. (1992) *Photosynthesis Res.* 31, 213–226.
- [10] Reddy, N.R.S., Small, G.J., Seibert, M. and Picorel, R. (1991) *Chem. Phys. Lett.* 1181, 391–399.
- [11] Reddy, N.R.S., Picorel, R. and Small, G.J. (1992) *Phys. Chem.* 196, 6458–6464.
- [12] Reddy, N.R.S., Cogdell, R., Zhao, L. and Small, G.J. (1993) *Photochem. Photobiol.* 157, 35–39.
- [13] van Mourik, F., Visschers, R.W. and van Grondelle, R. (1992) *Chem. Phys. Lett.* 193, 1–7.
- [14] van Mourik, F., Visschers, R.W. and van Grondelle, R. (1993) *Photochem. Photobiol.* 157, 19–23.